Journal of **A**pplied **B**iotechnology **R**eports

Original Article

Investigation on Crystallinity Behavior of the Polylactic Acid and Poly-3-hydroxybutyrate Bio-based Polymers in the Presence of the Pyromellitic Anhydride

Tayebeh Pourjafar Devin[1], Zahed Ahmadi[1*], Faramarz Afshari Taromi[2]

Abstract

Bio-based polymers have attracted significant attentions because of their renewable nature which can be a substitute of petroleum-based polymers; moreover, such polymers do not pollute the environment due to their degradable nature. In this research,the poly lactic acid (PLA) and poly-3-hydroxybutyrate (PHB) blend, as biodegradable polymers, behavior was investigated. Different ratios of PLA/PHB blend were prepared using solution casting method in the presence of the pyromellitic anhydride (PMDA) as acompatibilizer. DSC results revealed that the PMDA presence caused to separation of α-helix crystals and β-plate in two polymers resulting in phase separation via altering the crystallinity rate. PMDA can control the crystallization phenomenon which affected the crystallization rate, percentage and crystal size. Low molecular interaction was observed using the XRD results of pure and blended samples. SEM images of samples with higher content of PLA illustrated the homogeneous dispersion of PHB. Ring opening reaction of PMDA resulted in increasing the acidic number of samples which indicated the weak interaction with active group of polymers. It was observed no shit in IR peaks which indicated the incompatibility of these two polymers. Results shed light on the PMDA behavior in PLA/PHB blend which PMDA in spite of controlling the crystallinity behavior of the blend, cannot improve the compatibility and mixing.

1. Department of Chemistry, Amirkabir University of Technology, Tehran, Iran
2. Department of Polymer Engineering and Color Technology, Amirkabir University of Technology, Tehran, Iran

*** Corresponding Author**
Zahed Ahmadi
Department of Chemistry, Amirkabir University of Technology, Tehran, Iran
E-mail: zahmadi@aut.ac.ir

Submission Date: 6/2//2017
Accepted Date: 8/16/2017

Keywords: Polylactic Acid, Poly-3-hydroxybutyrate, Pyromellitic Anhydride, Crystallinity, Biodegradable polymers

Introduction

Eco-friendly features of biocompatible polymers has increased their usage in various application from electronic industry to biomedical applications [1]. Natural polymers have been used as a biocompatible and degradable polymer like alginate [2], chitosan [3] and agarose [4]. However, their poor properties leaded to use the synthetic biocompatible polymers like PLA [5] and PHB [6]. Nevertheless, such polymers still have some drawbacks. For improving such polymers properties various additives like Ag [7] and graphene oxide [8] have been added to endow special features like antibacterial properties. Grafting and copolymerization are the other remedy for increasing the biopolymers properties [9]. Blending has been proposed as a suitable and convenient method in which product can exhibit the synergic properties if the blended polymers have an appropriate compatibility [10, 11].

PLA is a biodegradable polymer with higher mechanical and physical properties than polyethylene terephthalate, polystyrene and polycarbonate. But sensitivity to thermal degradation in melt processing, low permeation resistance and flexibility, low stretching are its drawbacks [12]. PHB is a biodegradable polymer with high mechanical and physical properties similar to polypropylene, high permeation resistance and high thermal degradation temperature. PLA/PHB blends have attracted significant attention because their crystallinity and melting point are similar and cover each other drawbacks. Moreover, both of them can be degraded in environment with enzymatic reaction[13]. However, incompatibility of these polymers is one of the main hindrances for preparing this blend. Various methods and compatibilizers have been used for ameliorating the blend properties like PMDA [14] and organomodified clays [15].

Polyester as a plasticizer was added to the PLA/PHB blend to enhance the thermal and mechanical properties. Elongation at break of the PLA/PHB blend have improved significantly, moreover, degradation rate can be adjusted by altering the blend composition [16]. Cellulose nanocrystaline (CNC) was added to the PLA/PHB blends to improve its properties. CNC was modified with surfactant to enhance the interfacial adhesion to ameliorate the thermal stability. CNC along with crystallinity enhancement increased the processability and thermal degradation resistance [17]. Terpene d-limonene as a natural additive and plasticizer was added to the blend with dual aim to enhance the PLA crystallinity and improve the flexibility which such blend can be used as a food packaging film [18]. However, there is still remaining challenges about the relation between the mechanism of compatibility and crystallinity behavior of PLA/PHB blends.

In this research, it has been attempted to understand the mechanism of the effect of PMDA addition on the performance properties of the PLA/PHB blend. The results were obtained using a wide variety of techniques including FTIR, WAX, SEM and DSC to determine the PMDA ef-

fect on the compatibility between parent polymers in the PLA/PHB blend and its crystallinity behavior.

Materials and Methods

Materials

PLA grade 2003-D with density 1.24 g/cm^3, number-average molecular weight (Mn) 28878.3 g/mol, weight-avarage molecular weight 124305.9 (M_w) g/mol, and PDI 2.08 was purchased from NatureWorks LLC. PHB and PMDA were prepared from Biomer Company (Germany) and Merck Company. The materials were used without any purification.

Blend preparation

PLA/PHB blends have been prepared with different weight ratio (100/0, 75/25, 50/50, 0/100) were dissolved in chloroform solvent in the presence of the PMDA (1 and 0.5 wt. %) using the reflux method. after that the solution was casted and dried in oven at 50°C for solvent evaporation.

Characterization

Fourier transforms infrared spectroscopy (FTIR)

Sample characterized using FTIR spectroscopyusing Bruker apparatus in the ranges of 400-4000 cm^{-1} wavelength at room temperature.

Differential scanning calorimetry (DSC)

DSC (METTLER 822C) was utilized for evaluating the thermal and crystallinity behavior which the glass transition temperature (T_g), cold crystallization temperature (T_c), melting point (T_m), crystallinity percentage and the compatibility effect of PMDA. Heating rate was 10 °C/min and swept from -20 to 200°C. samples were remained at 200°C for 5 min to erase the thermal history, after that, samples were cooled to -20°C and heated again to 200°C. crystallinity degree was measured using equation 1.

$$X_c = \frac{\Delta H_m - \Delta H_{cc}}{w \Delta H_m^0} \qquad \text{Eq. 1}$$

Where, ΔH_m, $\Delta H_{cc}, X_c, w, \Delta H_m^0$ are the melting enthalpy, cold crystallization enthalpy, crystallization degree, weight percent and crystal melting enthalpy, respectively. ΔH_m^0 is 93 and j/g for PLA and PHB, respectively.

Wide angle X-ray diffraction (WAXD)

WAXD was performed using SIEMENS X-ray diffractometer (D5000, Germany) with Cobalt anode with 1200W power and 35kV with 30 mA at room temperature. 2θ degree was evaluated from 2 to 90 degree with 1.2 degree/min scanning rate. Bragg's law, nλ=2d sinθ, was used to compute the crystallographic spacing (d) of the samples. LaB6 as a calibration sample and BSE as a crystalline phase standard were utilized. XRD analysis has been used for qualitative and quantitative characterization of elements, anticipating the crystalline and amorphous phase, determining the network parameter and measuring the crystals percentage and size. Equation 2 is used for determining the crystallinity degree.

Xc(%)=1/(1+Ia/Ic).100
I(tot)=Ia+IcX- ra Eq. 2

where, Xc, Ia, Ic and I(tot) are crystallization percentage, amorphous under peak area, crystalline under peak area and total area, respectively [19].

Scanning electron Microscopy

SEM images were captured using Zeiss-Sigma apparatus (Germany). SEM images revealed that the particle size, phase dispersion/ratio; moreover, blend morphology and compatibility of PHB in PLA matrix were studied using SEM results. For this aim, micrometric films were immersed in boiling ethanol for 45 min to dissolve the PHB for evaluating the PHB footprint on PLA matrix [20].

Acidic number

Acidic number was used for determining the acidic hydroxyl groups in system which can be criterion for measuring the reaction process. ASTM-D1639-90 standard was used for this method. Coupling efficiency (CE) has been used for evaluating the reaction efficiency using the equation 3.

CE% = the number of coupled carboxylic end-group with chain-extenders/carboxy group of initial polymer *100

= the number of reduced end groups/ initial group * 100
= N_0-Nr/CV_0 *100 Eq. 3

Where, N_0, Nr are the end-group of the initial polymer and final polymer, respectively.

Results and Discussion

FTIR analysis was used for evaluating the reaction and chemical structure of blend. Figure 1 exhibits the FTIR peaks of PHB. Peaks around 1700-1750 cm^{-1} and 3200-3700 cm^{-1} are related to the vibration stretching carbonyl group and absorption stretching of hydroxyl group, respectively. The peak around 1710 cm^{-1} can be attributed to the PMDA grafting to the polyester of blend[21]. Stretching bond of C=O appears around 1720 cm^{-1} for PHB and 1746 cm^{-1} for PLA. Such peaks appear around 1721 and 1749 for blends. C-O-C stretching bond of crystalline sensitive which can attribute to the helix structure appear at 1225 and 1276 cm^{-1} for PHB, 1256 cm^{-1} for PLA and 1259 cm^{-1} for blends. PHB increment results in peak intensity enhancement [22]. Peaks around 1180, 1042 and 1128 cm^{-1} attribute to the C-O-C stretching bond of amorphous phase, vibration stretching of C-CH_3 and vibration rocking of CH_3 in PLA and PHB, respectively [23]. As it is clear from Fig. 1, CH_3 asymmetric deformation bond of PLA and PHB appear at 1359 and 1377 cm^{-1} which transfer to 1360 and 1379 in blends. The crystalline and amorphous peaks of PHB are observed at 855 and 895 cm^{-1}; moreover, such peaks are shown at 754 and 868 cm^{-1} for PLA. It is noteworthy that, these peaks appear in 755, 798 and 880 cm^{-1} for blend. There is no transfer was observed in blends peaks which any reaction do not occur with and without PMDA addition. Therefore, PLA and PHB are incompatible with/without PMDA.

As it was described in aforementioned section, the coupling efficiency which can be achieved by acidic number exhibits the reaction efficiency. The acidic number of blend is mentioned in Table 1.

Table 1 reveals that the acidic number of PHB is higher than that of PLA which PHB can potentially has higher activity. In spite of this fact, because of the higher crystallinity rate, PHB reactivity (esterification reaction) is low.

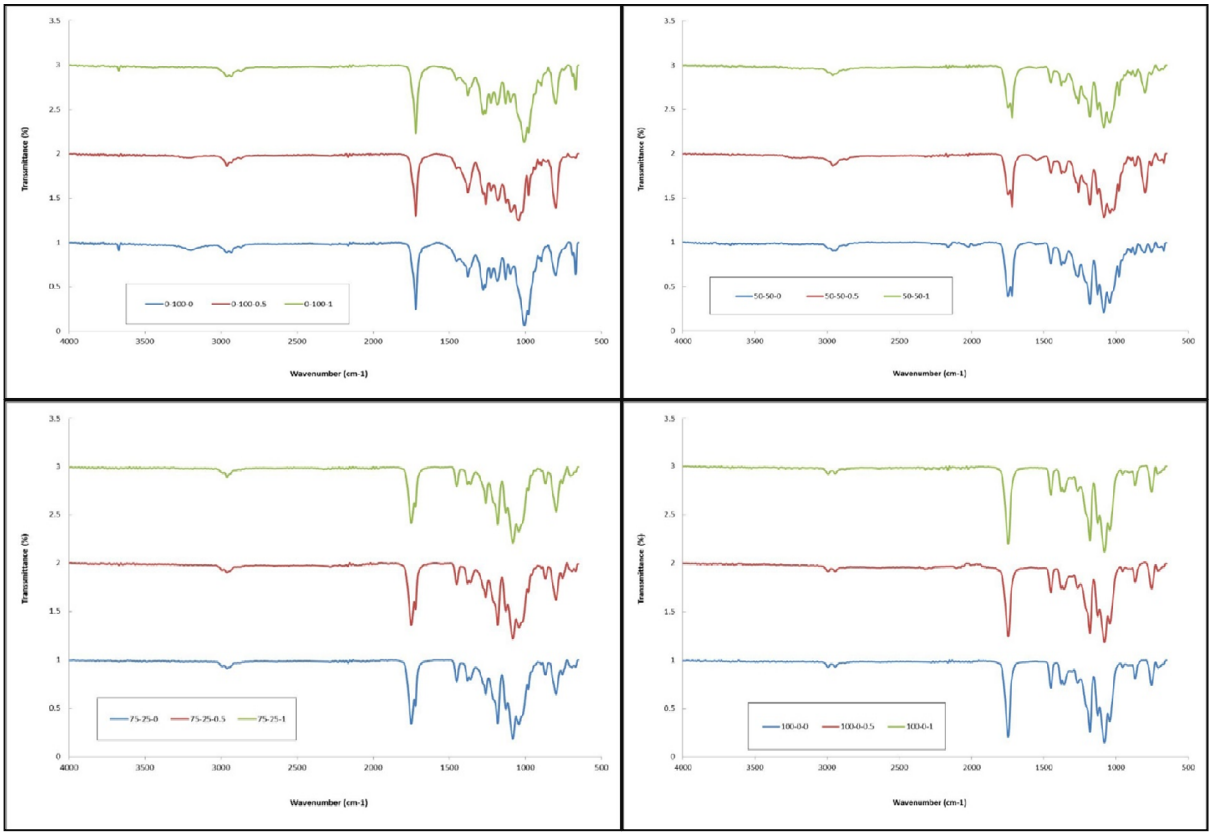

Figure 1. Blends FTIR peaks.

Table 1. Acidic number of different samples.

Blend	Acidic number	Blend	Acidic number
100/0/1	1.8469	75/25/1	102
100/0/0.5	8.311	75/25/0.5	80.142
100/0/0	20.543	75/25/0	33.512
50/50/1	148.412	0/100/1	228.904
50/50/0.5	107.471	0/100/0.5	167.562
50/50/0	16.1206	0/100/0	89.47

Pure PLA acidic number is 20.54 which with the presence of the PMDA, this number reduce to the 1 due to higher interaction of acidic groups and chain extender groups. On the other hand, high crystallinity rate of PHB cannot react with chain extender and consequently it degrades. During the reflux process, the transition of the anhydride group to the acidic group cause enhancement in acidic number [24].
DSC was utilized to evaluate the thermal behavior of blends. As it is obvious from Figure 2, T_g and T_m of the PLA is around 59 and 151.89^{o}C, respectively, which T_g of PLA reduces to 39^{o}C because of PHB addition and in next

Two different melting points indicate the two different crystallinity structures which can be obviously detectable in melting point of blends. Crystallization temperature is around 109^{o}C and there are no changes with PHB content enhancement but it is reduced with adding additives. Figure 2 revealed that the additive enhancement results in transferring the $T_g$and T_m to lower temperature. Additive involves the large chains in crystalline structure and short chains remain in amorphous phase. Different melting points are observed in blend which can be related to the recrystallization or different lamellar thickness [25]. Dif-

ferent melting points indicate the different crystalline structure. Ikehara *et al.*, explained that the crystallization behavior of two polymers in blend strongly depends on the melting point differences.

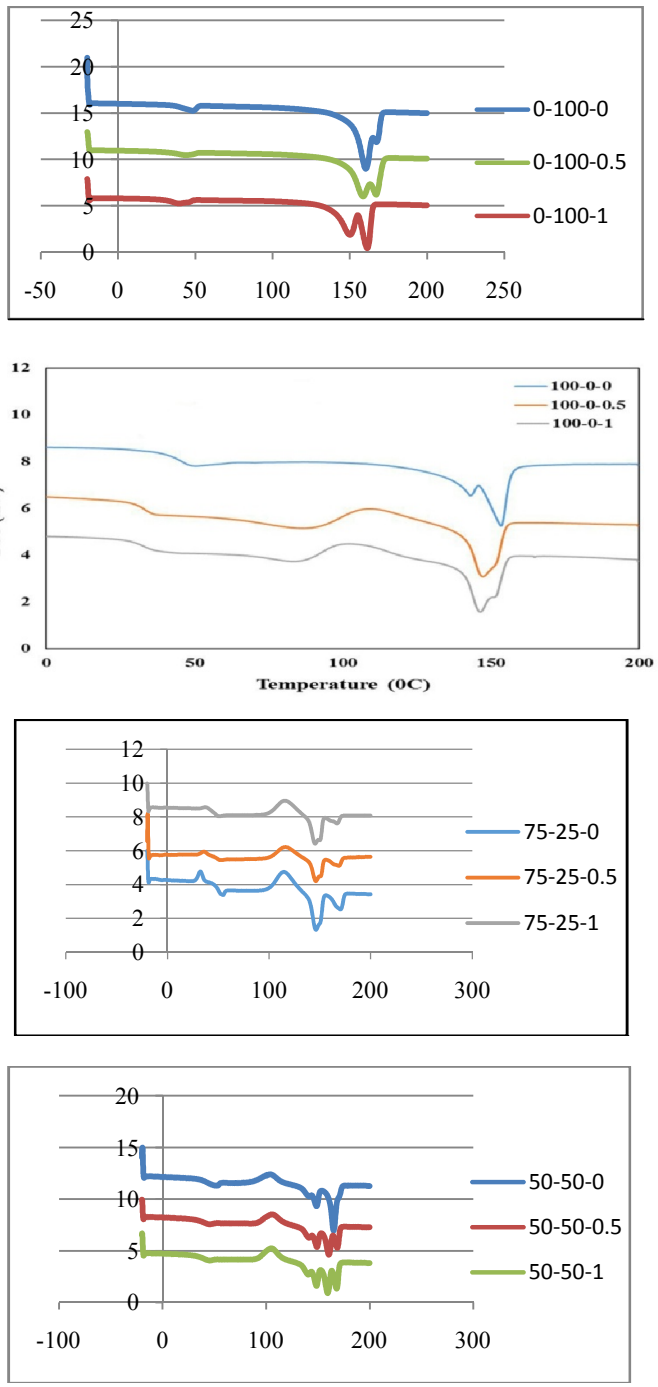

Figure 2. DSC peaks of PLA-PHB Blends in the presence of PMDA.

In high differences, the component with higher melting point initiates the crystallization and form the spherolite, after that, the other polymer's crystals juxtapose the formed crystals.

In low melting point differences, each one crystallizes individually. In this research, the melting point between PHB and PLA was around 10°C which everyone initiated crystallization process solitarily. The two melting points presence in blend proved this hypothesis. Figure 2 exhibits the two separated melting point at 148 and 165°C for PHB in 50/50/0 composition of blend and the peak at 141°C attributes to PLA. 0.5 wt. % addition a of additive cause to transfer the melting point to 149 and 169°C but the PLA melting point remains constant. 1 wt. % of additive addition to the blend results in achieve two melting points. In 75-25-0 composition, two melting points at 150 and 170°C for PHB and 146°C for PLA are obvious. Remelting process or different lamellar structure cause to observes two melting points in some samples. The effect of additive on PLA was higher than PHB because of the more variation in PLA crystallinity behavior.

In pristine PHB, bimodal melting point is detectable at 160 and 167°C related to α and β spherolite. Addition of 0.5 wt. % of PMDA to the blend causes the melting point shift to 158 and 167°C. 1 wt. % addition of PMDA causes the melting point shifts to 150 and 161°C and the intensity of peaks was changed. These results indicated that the PMDA enhancement affect the crystallinity behavior and structure directly and separated α and β plates. PDMA addition resulted in phase separation because of changing the crystallization rate; hence, this additive was effective for controlling the crystallization rate, crystallinity percentage and crystal size [26, 27].

Crystallization rate of PHB was high and it was crystalline before the PMDA can affect the compatibility and PHB do not participate in the reaction. But, PMDA because of the lower crystallinity rate of PLA can affect the PLA crystallinity behavior. PHB presence in samples resulted in higher crystallinity because of its higher crystallinity rate. PHB cannot affect the crystallinity behavior of PLA but PMDA affect the PLA crystallinity behavior. Orthorhombic structure was observed in PHB crystalline structure because of its high crystallinity rate. Amorphous phase resulted in widening the peaks and the crystalline area was suitable for study. PHB network parameters were a = 0.575 nm and b = 1.312 nm with left-handed 21 helix chain conformation [28]. PLA can crystalize from melt/solution state within orthorhombic structure with a = 1.037 and b = 0.598 [16] which can be observed two kind of crystalline structure (α and β), α structure forms as a helical shape 10_3 and β structure forms as a spiral shape 3_1. PHB usually exhibit two refraction peaks around 13.5° and 16.8° accordance with crystalline plates and three weak peaks was observed around 19.1°, 22.2° and 25.5° attributing to the orthorhombic structure. Figure 3 exhibits the 2 peaks around 15.45 and 19.46 relating to the PHB in the presence of the chain extender and PLA blend. Reduction of the peaks intensity indicated that the orientation of crystalline plates varied with PMDA presence and crystallinity growth was hindered with composition enhancement. Network parameters and their location remained constant indicating the orthorhombic crystals were not changed. The position constancy of peaks showed that the chain extender cannot affect the orthorhombic structure but affect the crystals orientation. Moreover, PLA cannot affect the crystals structure. SEM images were captured for evaluating the surface properties of PLA/PHB blend. Figure 4 revealed that the appropriate

dispersion of PHB in PLA matrix (75/25/0). The pores indicate the PHB solving in ethanol during etching process.

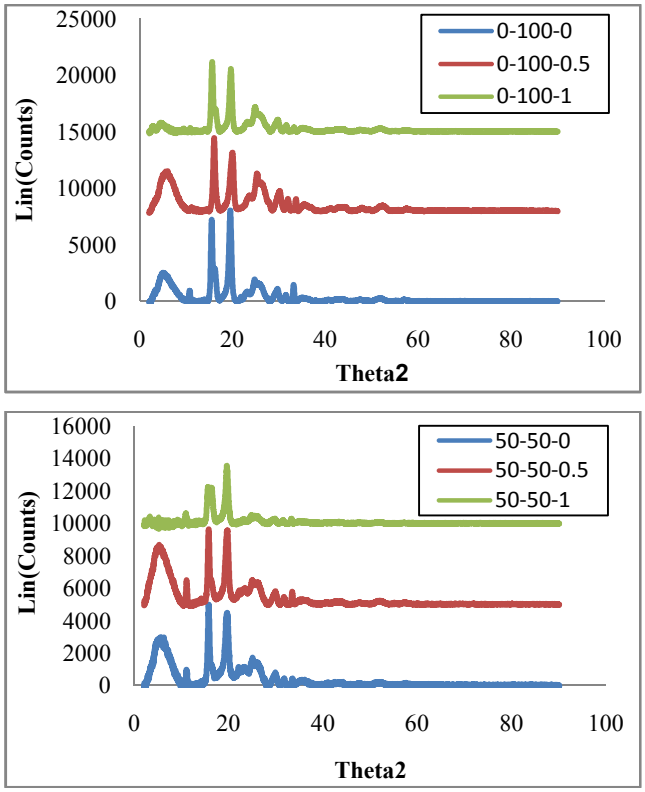

Figure 3. WAXD test of PLA/PHB/PMDA blends.

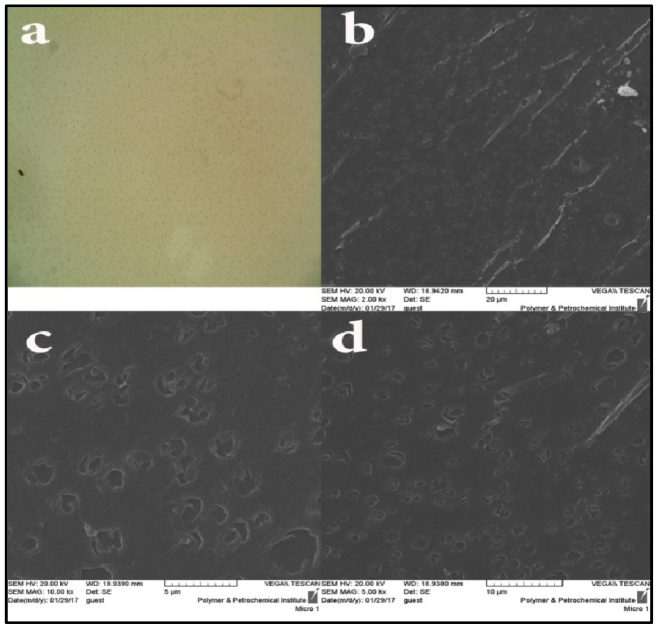

Figure 4. Images of 75/25/0 blend in the presence of the methanol. a) with optical microscope. b, c, & d) different scales with SEM.

Samples film was form on the glass surface and immersed in methanol to dissolve the amorphous PHB. PLA remained untouched and the pores were formed on its surface because of amorphous PHB dissolving (Figure 5).

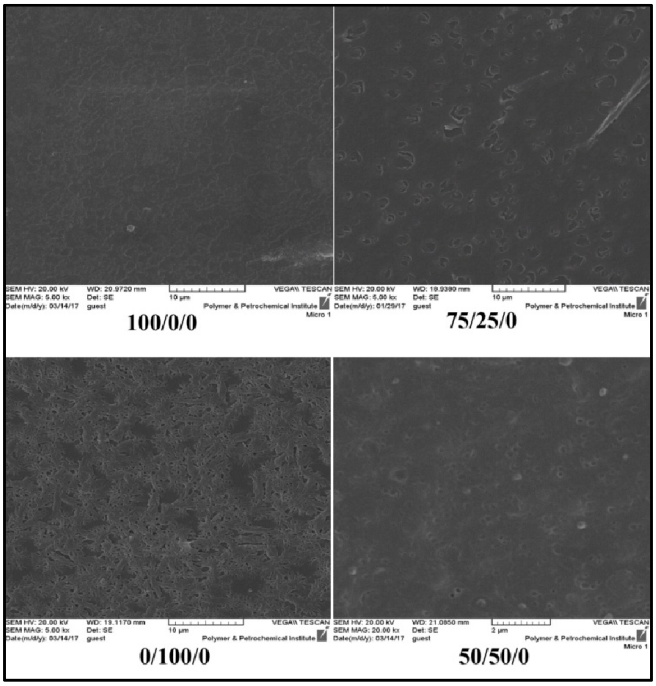

Figure 5. SEM image of etched film of blend 100/0/0, 75/25/0, 0/100/0, 50/50/0.

Figure 6 and 7 reveals that the PMDA cannot enter within the polymer substrate and interact properly; consequently, PMDA has no effect on compatibility and molecular weight enhancement. On the other hand, it changes the crystallinity pattern and result in dendritic structure.

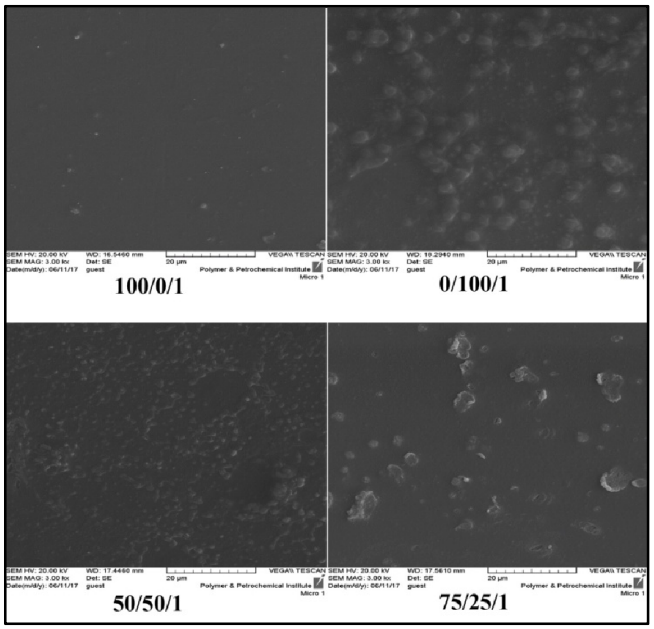

Figure 6.Etched film in presence of 1 wt.% PMDA.

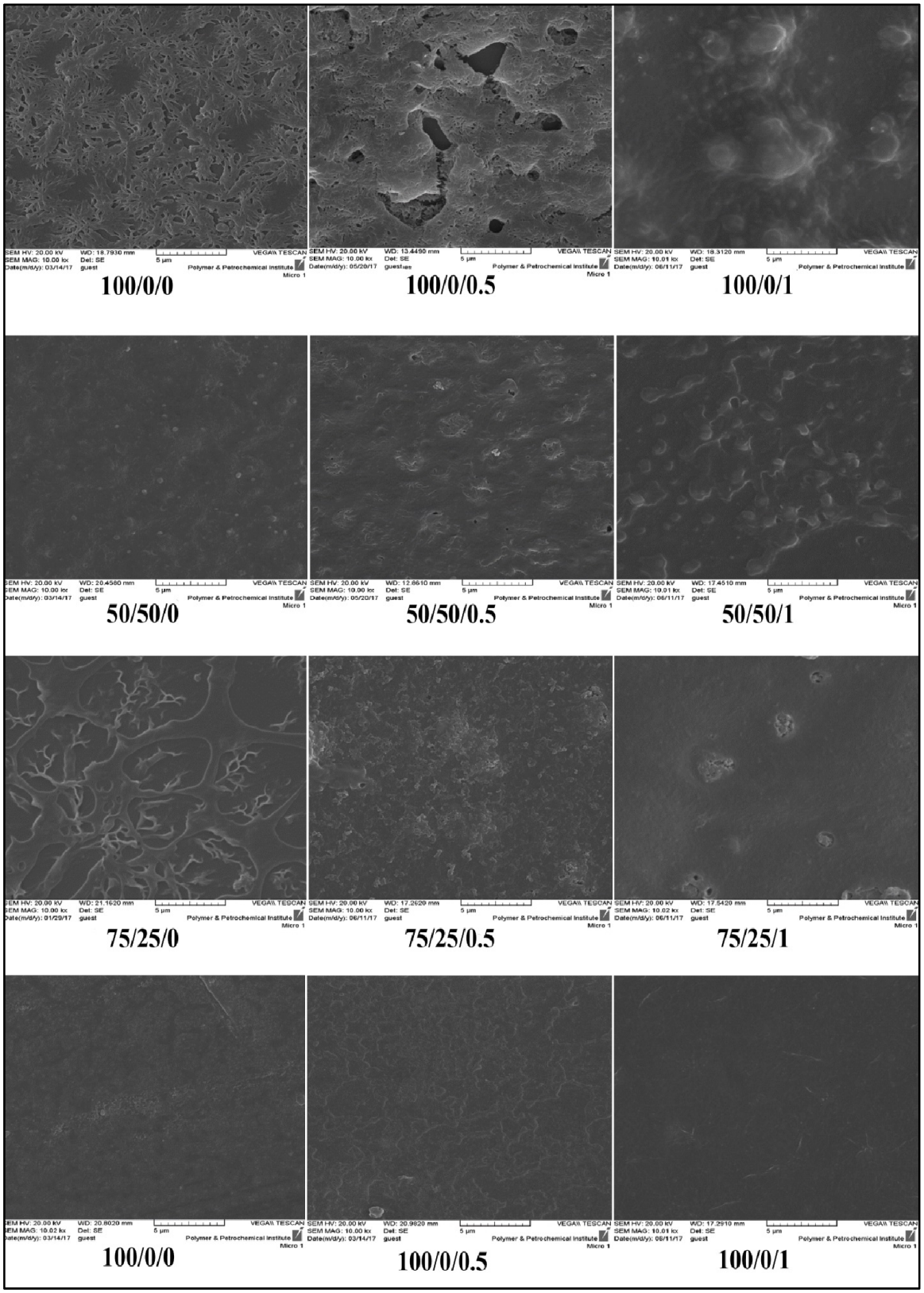

Figure 7. Effect of PMDA on crystalline structure.

Conclusion

In this study, the effect of the PMDA was evaluated on the PLA/PHB blends. Structure, morphology of crystallization, melting behavior and compatibility of PLA/PHB was investigated. It was revealed that PHB has two crystalline structures (α, β) while PLA has one crystalline structure with low crystallization rate. Blend composition and additives can affect the crystallinity structure like spherulite growth pattern. Form DSC results it was concluded that the, additive can affect the PLA crystalline structure because of the low crystallization rate. Additive addition caused the separation of α-helix and β-plates which can separate phases because it varied the crystallization rate; therefore, PMDA can affect the crystallization rate, behavior and crystal sizes but it was not suitable for compatibilization due to the high crystallization rate of PHB. XRD test exhibited the presence of four peaks of α crystal attributed to 121, 110, 020 and 040 and one peak of β crystal attribute to 021 which was the network parameter of the pure polymer. Constancy of these parameters indicated that the additive affect the crystallinity behavior of each part but cannot affect the compatibility of PLA and PHB.

Acknowledgements

The authors would like to thank colleagues for their kind and generous assistance.

References

1. Zarrintaj, P., Moghaddam, A.S., Manouchehri, S., Atoufi, Z., Amiri, A., Amirkhani, M.A., Nilforoushzadeh, M.A., Saeb, M.R., Hamblin, M.R., Mozafari, M., Can regenerative medicine and nanotechnology combine to heal wounds? The search for the ideal wound dressing. *Nanomedicine*, 2017, Vol. 12, pp. 2403-2422.

2. Atoufi, Z., Zarrintaj, P., Motlagh, G.H., Amiri, A., Bagher, Z., Kamrava, S.K., A novel bio electro active alginate-aniline tetramer/agarose scaffold for tissue engineering: synthesis, characterization, drug release and cell culture study. *J Biomater Sci, Polym Ed*, 2017, Vol. pp. 1-43.

3. Rahmati, M., Milan, P.B., Samadikuchaksaraei, A., Goodarzi, V., Saeb, M.R., Kargozar, S., Kaplan, D.L., Mozafari, M., Ionically crosslinked thermoresponsive chitosan hydrogels formed in situ: A conceptual basis for deeper understanding. *Macromol Mater Eng*, 2017, Vol. 302, pp. 1-7.

4. Zarrintaj, P., Bakhshandeh, B., Rezaeian, I., Heshmatian, B., Ganjali, M.R., A novel electroactive agarose-aniline pentamer platform as a potential candidate for neural tissue engineering. *Sci Rep*, 2017, Vol. 7, pp. 17186-17189.

5. Yazdanpanah, A., Tahmasbi, M., Amoabediny, G., Nourmohammadi, J., Moztarzadeh, F., Mozafari, M., Fabrication and characterization of electrospun poly-L-lactide/gelatin graded tubular scaffolds: Toward a new design for performance enhancement in vascular tissue engineering. *Prog Nat Sci: Mater Int*, 2015, Vol. 25, pp. 405-413.

6. Deepthi, S., Sundaram, M.N., Vijayan, P., Nair, S.V., Jayakumar, R., Engineering poly (hydroxy butyrate-co-hydroxy valerate) based vascular scaffolds to mimic native artery. *Int J Boil Macromol*, 2018, Vol. 109, pp. 85-98.

8. Hafshejani, T.M., Zamanian, A., Venugopal, J.R., Rezvani, Z., Sefat, F., Saeb, M.R., Vahabi, H., Zarrintaj, P., Mozafari, M., Antibacterial glass-ionomer cement restorative materials: A critical review on the current status of extended release formulations. *J ControlRelease*, 2017, Vol. 262, pp. 317-328.

9. Nonahal, M., Rastin, H., Saeb, M.R., Sari, M.G., Moghadam, M.H., Zarrintaj, P., Ramezanzadeh, B., Epoxy/PAMAM dendrimer-modified graphene oxide nanocomposite coatings: Nonisothermal cure kinetics study. *Prog Org Coat*, 2018, Vol. 114, pp. 233-243.

10. Zarrintaj, P., Urbanska, A., Gholizadeh, S.S., Goodarzi, V., Saeb, M.R., Mozafari, M., A facile route to the synthesis of anilinic electroactive colloidal hydrogels for neural tissue engineering applications. *J Colloid Interface Sci*, 2018, Vol. 516, pp. 57-66.

11. Tavakoli Anaraki, F., Saeb, M.R., Rastin, H., Ghiyasi, S., Khonakdar, H.A., Goodarzi, V., Khalili, R., Mostafapoor, F., Jafari, S.H., A probe into the status quo of interfacial adhesion in the compatibilized ternary blends with core/shell droplets: Selective versus dictated compatibilization. *J Appl Polym Sci*, 2017, Vol. 134, pp. e45503-

12. Sari, M.G., Saeb, M.R., Shabanian, M., Khaleghi, M., Vahabi, H., Vagner, C., Zarrintaj, P., Khalili, R., Paran, S.M.R., Ramezanzadeh, B., Epoxy/starch-modified nano-zinc oxide transparent nanocomposite coatings: A showcase of superior curing behavior. *Prog Org Coat*, 2018, Vol. 115, pp. 143-150.

12. Auras, R., *Poly (lactic acid)*. 2010: Wiley Online Library.

13. Moorkoth, D., Nampoothiri, K.M., Production and characterization of poly (3-hydroxy butyrate-co-3 hydroxyvalerate) (PHBV) by a novel halotolerant mangrove isolate. *Bioresour Technol*, 2016, Vol. 201, pp. 253-260.

14. Wang, W., Yu, K., Zhou, H., Wang, X., Mi, J., The Effect of Compatibilization on the Properties and Foaming Behavior of Poly (ethylene terephthalate)/Poly (ethylene-octene) Blends. *Cell Polym*, 2017, Vol. 36, pp. e313.

15. Paran, S.M.R., Abdorahimi, M., Shekarabi, A., Khonakdar, H.A., Jafari, S.H., Saeb, M.R., Modeling and analysis of nonlinear elastoplastic behavior of compatibilized polyolefin/polyester/clay nanocomposites with emphasis on interfacial interaction exploration. *Compos Sci Technol*, 2018, Vol. 154, pp. 92-103.

16. Abdelwahab, M.A., Flynn, A., Chiou, B.S., Imam, S., Orts, W., Chiellini, E., Thermal, mechanical and morphological characterization of plasticized PLA–PHB blends. *Polym Degrad Stab*, 2012, Vol. 97, pp. 1822-1828.

17. Arrieta, M., Fortunati, E., Dominici, F., Rayón, E., López, J., Kenny, J., Multifunctional PLA–PHB/cellulose nanocrystal films: processing, structural and thermal properties. *Carbohydrate polym*, 2014, Vol. 107, pp. 16-24.

18. Arrieta, M.P., López, J., Hernández, A., Rayón, E., Ternary PLA–PHB–Limonene blends intended for biodegradable food packaging applications. *Eur Polym J*, 2014, Vol. 50, pp. 255-270.

19. Mahmodi, G., Sharifnia, S., Madani, M., Vatanpour, V., Photoreduction of carbon dioxide in the presence of H 2, H 2 O and CH 4 over TiO 2 and ZnO photocatalysts. *Sol Energy*, 2013, Vol. 97, pp. 186-194.

20. Mahmodi, G., Sharifnia, S., Rahimpour, F., Hosseini, S., Photocatalytic conversion of CO_2 and CH_4 using ZnO coated mesh: effect of operational parameters and optimization. *Sol Energy Mater Sol Cell*, 2013, Vol. 111, pp. 31-40.

21. Wu, C.S., Assessing biodegradability and mechanical, thermal, and morphological properties of an acrylic acid-modified poly (3-hydroxybutyric acid)/wood flours biocomposite. *J Appl Polym Sci*, 2006, Vol. 102, pp. 3565-3574.

22. Furukawa, T., Sato, H., Murakami, R., Zhang, J., Duan, Y.-X., Noda, I., Ochiai, S., Ozaki, Y., Structure, dispersibility, and crystallinity of poly (hydroxybutyrate)/poly (L-lactic acid) blends studied by FT-IR microspectroscopy and differential scanning calorimetry. *Macromol*, 2005, Vol. 38, pp. 6445-6454.

23. Hu, Y., Sato, H., Zhang, J., Noda, I., Ozaki, Y., Crystallization behavior of poly (L-lactic acid) affected by the addition of a

small amount of poly (3-hydroxybutyrate). *Polymer*, 2008, Vol. 49, pp. 4204-4210.
24. Iriondo, P., Iruin, J., Fernandez-Berridi, M., Association equilibria and miscibility prediction in blends of poly (vinylphenol) with poly (hydroxybutyrate) and related homo-and copolymers: an FTIR study. *Macromol*, 1996, Vol. 29, pp. 5605-5610.
25. Gunaratne, L., Shanks, R., Miscibility, melting, and crystallization behavior of poly (hydroxybutyrate) and poly (D, L-lactic acid) blends. *Polym Eng Sci*, 2008, Vol. 48, pp. 1683-1692.
26. Chen, L., Wang, M., Production and evaluation of biodegradable composites based on PHB–PHV copolymer. *Biomaterials*, 2002, Vol. 23, pp. 2631-2639.
27. Galego, N., Rozsa, C., Sánchez, R., Fung, J., Vázquez, A.a., Santo Tomás, J., Characterization and application of poly (β-hydroxyalkanoates) family as composite biomaterials. *Polym Test*, 2000, Vol. 19, pp. 485-492.
28. El-Hadi, A.M., Effect of processing conditions on the development of morphological features of banded or nonbanded spherulites of poly (3-hydroxybutyrate) (PHB) and polylactic acid (PLLA) blends. *Polym Eng Sci*, 2011, Vol. 51, pp. 2191-2202.